Helminth induced monocytosis conveys protection from respiratory syncytial virus infection in mice.

Matthew Burgess O[1], Piotr Janas[1], Karla Berry[1], Hannah Mayr[2], Matthias Mack[3], Stephen Jenkins J[1], Calum Bain C[1], Henry J. McSorley[4], and Jürgen Schwarze[1]

[1]The University of Edinburgh Centre for Inflammation Research
[2]Medizinische Universitat Wien
[3]Universitat Regensburg
[4]University of Dundee Division of Cell Signalling and Immunology

May 11, 2023

Abstract

Background Respiratory syncytial virus (RSV) infection in infants is a major cause of viral bronchiolitis and hospitalisation. We have previously shown in a murine model that ongoing infection with the gut helminth *Heligmosomoides polygyrus* (*H. polygyrus*) protects against RSV infection through type I interferon (IFN-I) dependent reduction of viral load. Yet, the cellular basis for this protection has remained elusive. Given that recruitment of mononuclear phagocytes to the lung is critical for early RSV infection control, we assessed their role in this coinfection model. **Methods** Mice were infected by oral gavage with *H. polygyrus*. Myeloid immune cell populations were assessed by flow cytometry in lung, blood and bone marrow throughout infection and after secondary infection with RSV. Monocyte numbers were depleted by anti-CCR2 antibody or increased by intravenous transfer of enriched monocytes. **Results** *H. polygyrus* infection induces bone marrow monopoiesis, increasing circulatory monocytes and lung mononuclear phagocytes in a IFN-I signalling dependent manner. This expansion causes enhanced lung mononuclear phagocyte counts early in RSV infection that may contribute to the reduction of RSV load. Depletion or supplementation of circulatory monocytes prior to RSV infection confirms that these are both necessary and sufficient for helminth induced antiviral protection. **Conclusions** *H. polygyrus* infection induces systemic monocytosis contributing to elevated mononuclear phagocyte numbers in the lung. These cells are central to an anti-viral effect that reduces the peak viral load in RSV infection. Treatments to promote or modulate these cells may provide novel paths to control RSV infection in high risk individuals.

Title:

Helminth induced monocytosis conveys protection from respiratory syncytial virus infection in mice.

Short title:

Helminth induced monocytes reduce RSV load.

Authors:

Matthew O Burgess$_1$ Piotr Janas$_1$ Karla Berry$_1$ Hannah Mayr$_1$ Matthias Mack$_2$ Stephen J Jenkins$_1$ Calum C Bain$_1$ Henry J McSorley$_3$ Jurgen Schwarze$_{1,\ 4}$

Author's affiliations:

1 Centre for Inflammation Research, University of Edinburgh, United Kingdom. 2 Department of Nephrology, University Hospital Regensburg, Germany. 3 Cell signalling and Immunology, School of Life Sciences, University of Dundee, United Kingdom, 4 Child Life and Health, University of Edinburgh, United Kingdom.

Correspondence address for Hannah Mayr is now Institute of Medical Genetics, Medical University of Vienna, Austria.

Acknowledgments:

Study design by MOB, SJJ, CBB, HJMcS and JS. Experiments performed by MOB with PJ, KB for flow cytometry and with HM for Methocult assays. MOB, CCB and HJMcS analysed and discussed the data. MOB and JS drafted the manuscript and MOB, HM, SJJ, CCB, HJMcS and JS critically reviewed and revised the manuscript. JS obtained the funding. MM developed and provided the MC-21 antibody. All authors gave final approval to the version submitted for publication.

Flow cytometry data was generated with support from the QMRI Flow Cytometry and cell sorting facility, University of Edinburgh. This work was funded by UKRI-MRC grant MR/T029668/1. This UK funded award is part of the EDCTP2 programme supported by the European Union. CCB is supported by a Sir Henry Dale Fellowship jointly funded by the Wellcome Trust and the Royal Society (grant number 206234/Z/17/Z). We thank Amy Buck (University of Edinburgh, United Kingdom) for providing *H. polygyrus* L3 larvae and Samanta Mariani (University of Edinburgh, United Kingdom) for advice on bone marrow Methocult assays.

Abstract:

Background Respiratory syncytial virus (RSV) infection in infants is a major cause of viral bronchiolitis and hospitalisation. We have previously shown in a murine model that ongoing infection with the gut helminth *Heligmosomoides polygyrus* (*H. polygyrus*) protects against RSV infection through type I interferon (IFN-I) dependent reduction of viral load. Yet, the cellular basis for this protection has remained elusive. Given that recruitment of mononuclear phagocytes to the lung is critical for early RSV infection control, we assessed their role in this coinfection model.

Methods Mice were infected by oral gavage with *H. polygyrus* . Myeloid immune cell populations were assessed by flow cytometry in lung, blood and bone marrow throughout infection and after secondary infection with RSV. Monocyte numbers were depleted by anti-CCR2 antibody or increased by intravenous transfer of enriched monocytes.

Results *H. polygyrus* infection induces bone marrow monopoiesis, increasing circulatory monocytes and lung mononuclear phagocytes in a IFN-I signalling dependent manner. This expansion causes enhanced lung mononuclear phagocyte counts early in RSV infection that may contribute to the reduction of RSV load. Depletion or supplementation of circulatory monocytes prior to RSV infection confirms that these are both necessary and sufficient for helminth induced antiviral protection.

Conclusions *H. polygyrus* infection induces systemic monocytosis contributing to elevated mononuclear phagocyte numbers in the lung. These cells are central to an anti-viral effect that reduces the peak viral load in RSV infection. Treatments to promote or modulate these cells may provide novel paths to control RSV infection in high risk individuals.

Keywords:

Helminth, Innate immunity, Mononuclear phagocyte, RSV, Virus

Main Text:

Introduction

Respiratory syncytial virus (RSV) induced viral bronchiolitis is a major cause of infant hospitalisation worldwide[1]. Adult infection is frequently associated with mild respiratory illness but can also cause significant morbidity and mortality in the elderly and immunocompromised individuals[2,3]. There is as yet no active vaccination towards or specific therapy for RSV infection although many promising candidates are currently in clinical trials. Treatment is limited to supportive measures and prophylaxis for high risk infants with the anti-RSV F-protein antibody palivizumab, a high cost option with limited effectiveness[4,5].

Novel approaches to managing RSV, and greater understanding of the immune response to infection, are still required. We have previously reported that an ongoing infection with the murine enteric helminth*Heligmosomoides polygyrus* (*H. polygyrus*) is able to improve RSV infection outcomes by suppressing the peak viral load early in infection[6]. This work found that the adaptive immune response to *H. polygyrus* infection, the type 2 immune response, characteristic of helminthic infection and typified by robust IL-33, IL-4 and IL-13 signalling[7], as well as the anti-microbial peptide LL-37 are not required for the *H. polygyrus* induced anti-viral immunity in the lung. Rather, type I interferon (IFN-I) signalling, induction of interferon beta (IFNβ) and interferon stimulated genes (ISGs), including *Rsad2* (encoding viperin) and *Oas1a* are central to the *H. polygyrus* induced protective effect against RSV infection. Many ISGs have antiviral functions and both viperin and OAS can limit RSV infection[8,9]. Almost all cells of the lung have the capacity to both produce one or more of the family of IFN-Is and to respond to IFN-I signalling through the dedicated receptor IFNalpha receptor (IFNAR) [10-12]. This broad potential space for IFN-I signalling led us to question which cells may be contributing to*H. polygyrus* induced anti-viral effects. Mononuclear phagocytes, including monocytes and macrophages, are known responders to IFN-Is and have been linked to early control of RSV infection[13,14]. IFN-Is can regulate monocyte recruitment during inflammation, skew hematopoietic output, and through interferon regulatory factors promote differentiation to, and polarisation of, macrophages[15-18]. Monocytes can also be potent produces of IFN-Is, especially IFNβ, in response to stimuli including RSV[19]. We therefore hypothesised that lung mononuclear phagocytes following *H. polygyrus* infection mediate the helminth induced protective effect against RSV infection.

Materials and Methods

Animals

BALB/c mice were purchased from Charles River (Margate, Kent, UK). C57BL/6 and *Ifnar1*$^{-/-}$ (C57BL/6 background)[20] mice were bred in-house at the University of Edinburgh. Eight – 12 week old mice were infected by oral gavage with 200 stage 3 *H. polygyrus* larvae. Some animals were administered 20 μg of anti-CCR2 antibody (MC-21, gift M. Mack) by intra-peritoneal injection seven and nine days later. Other animals were given 2x10^6 enriched bone marrow monocytes by intravenous injection. Some animals were infected with RSV (10^{5}plaque forming units) intranasally ten days after *H. polygyrus*infection. After monocyte transfer RSV was administered 30 minutes later. All procedures were approved by local ethical review committee and the UK Home Office.

Parasites and viral stocks

The parasite life cycle was maintained as previously described[21]. Plaque-purified human RSV (Strain A2; ATCC, VA, USA) was grown in HEp-2 cells as previously described[22].

RSV immunoplaque assay

RSV titres were assessed by immunoplaque assay. Lung homogenates were titrated onto HEp-2 cell monolayers in 96-well plates. Twenty-four hours later monolayers were fixed and permeabilised with 2% H_2O_2 in methanol then bound with biotin-conjugate goat anti-RSV antibody (BioRad; Watford, Hertfordshire, UK). Plaques were visualised with extravadin peroxidase and AEC red (SigmaAldrich; Glasgow, Scotland, UK) and infection units observed by light microscopy.

L-gene real time PCR

Lungs were homogenized in 1 mL of TRIzol (ThermoFisher Scientific; Waltham, MA, USA). cDNA was made from the two μg extracted RNA using HC cDNA RT kit (ThermoFisher Scientific; Waltham, MA, USA) according to manufacturer's instructions. Custom primers and probe for RSV L gene were used as previously described[6].

Colony forming assays

Bone marrow colony forming assays were performed with MethoCult GF M3434 (StemCell Technologies; Cambridge, Cambridgeshire, UK) per manufacturer's instructions. Bone marrow from hind limb tibia and

femur flushes was washed, 70 μM filtered and then resuspended in MethoCult GF M3434 at 1x10^4 cells per 35mm culture dish in duplicate. Plates were incubated at 37°C 5% CO_2 in humidified chambers. After 10-12 days colonies were characterised to lineage and counted.

Flow cytometry

Following digestion with Liberase (385μg/mL PBS; SigmaAldrich; Glasgow, Scotland, UK) and DNaseI (0.5mg/mL; SigmaAldrich; Glasgow, Scotland, UK) and red blood cell lysis (Hybrimax buffer; SigmaAldrich; Glasgow, Scotland, UK) 2x10^6 lung cells per panel were stained with LIVE/DEAD fixable near-IR dead cell kit (ThermoFisher Scientific; Waltham, MA, USA). The following anti-mouse antibodies were used for immune cell characterisation; Brilliant Violet 510 CD11c (N418; Biolegend; London, UK), Brilliant Violet 570 CD11b (M1/70; Biolegend; London, UK), Brilliant Violet 605 CD45 (30-F11; Biolegend; London, UK), AlexaFluor 647 CD64 (X54-5/7.1; Biolegend; London, UK), AlexaFluor 700 Ly6C (HK1.4; Biolegend; London, UK), phycoerythrin Siglec-F (E50-2440; BD Biosciences; Wokingham, Berkshire, UK), eFluor 450 Ly6G (1A8; ThermoFisher Scientific; Waltham, MA, USA). Fc-receptor binding was blocked using anti-mouse CD16/CD32 antibody (2.4G2) (BD Biosciences; Wokingham, Berkshire, UK).

Red blood cell were lysed (RBC lysis buffer; Biolegend; London, UK) and 50 μl per panel was stained with dead cell kit as above and the following antibodies used; Lineage dump (Brilliant Violet 421 Siglec F (E50-2440; BD Biosciences), Pacific Blue CD3 (17A2; Biolegend; London, UK), CD19 (6D5; Biolegend; London, UK), and CD49b (PK136; Biolegend; London, UK)), Brilliant Violet 510 Ly6G (1A8; Biolegend; London, UK), Brilliant Violet 605 CD45 (30-F11; Biolegend; London, UK), Brilliant Violet 650 CD11b (M1/70; Biolegend; London, UK), phycoerythrin Treml4 (16E5; Biolegend; London, UK), allophycocyanin CD115 (AFS98; Biolegend; London, UK), AlexaFluor 700 Ly6C (HK1.4; Biolegend; London, UK). Fc-receptor binding was blocked as above.

2x10^6 bone marrow cells were stained with dead cell kit as above, lineage dump (as above plus Pacific Blue Ly6G (1A8; Biolegend; London, UK), TER-119 (TER-119; Biolegend; London, UK), CD11c (N418; Biolegend; London, UK)), BV711 CD16/CD32 (93; Biolegend; London, UK), PE-Cy7 CD117 (2B8; Biolegend; London, UK), allophycocyanin CD115 (AFS98; Biolegend; London, UK) and AlexaFluor 700 Ly6C (HK1.4; Biolegend; London, UK). Fc-receptor binding was blocked using purified mouse serum (M5905; SigmaAldrich; Glasgow, Scotland, UK).

Flow cytometry samples were analysed with an Aurora cytometer (Cytek; Amsterdam, The Netherlands) and analysis performed with FCS Express 7 (De Novo Software; Pasadena, CA, USA).

Monocyte isolation

To enrich bone marrow monocytes for cell transfer experiments mouse monocyte isolation Kit (130-100-629; Miltenyl Biotec; Bisley, Surrey, UK) was used.

Statistical analysis

All data were analysed using Prism 9 software (GraphPad Software; Boston, MA, USA). Data from two groups were analysed by unpaired*t* test, while data from more than two groups were analysed by one-way ANOVA with Tukey's multiple comparisons test with a single pooled variance. Unless otherwise stated, differences are statistically non-significant. **** p <0.0001, *** p<0.001; ** p <0.01; * p<0.05.

Results

H. polygyrus infection induces blood monocytosis and increases lung mononuclear phagocytes .

The early response to RSV infection in mice drives the recruitment of monocytes to the lung causing an accumulation of mononuclear phagocytes[13]. In the initial hours of infection these cells are predominantly $Ly6C^{hi}$, later downregulating Ly6C and becoming predominantly $CD11c^{+}$. Flow cytometric analysis was used to assess if these populations were also affected by *H. polygyrus* infection. Female Balb/c mice were infected with *H. polygyrus* and lungs assessed for innate immune cell composition through the later stages of

infection. Cells of the monocyte-macrophage lineage were identified by their expression of the high affinity Fc receptor, CD64 (also known as FcγR1), and subdivided on the basis of SiglecF expression. SiglecF expressing CD64$^+$ cells represent alveolar macrophages, whereas the SiglecF$^-$ compartment will contain interstitial macrophages and some monocytes and their progeny. Compared with sham infection controls there was an increase in the numbers of mononuclear phagocytes (CD45$^+$, Ly6G$^-$, SiglecF$^-$, CD11b$^+$, CD64$^+$, Fig. 1A) in the lungs of *H. polygyrus*infected mice from ten days post infection, subsiding yet still elevated at 14 days. (Fig. 1B). In comparison, the resident alveolar macrophage compartment (CD45$^+$, Ly6G$^-$, SiglecF$^+$, CD11b$^-$, CD64$^+$, Fig. 1A) remained unchanged (Fig. 1C). The expansion was predominantly due to Ly6C$^+$ macrophages with a variable increase in CD11c$^+$ only at day ten (Fig. 1D-F).

A large proportion of the recruited macrophages seen in response to lung inflammatory stimuli are derived from circulating monocytes[23,24]. It is therefore likely that the vascular monocyte reservoir would reflect the observed influx of mononuclear phagocytes to the lung. Peripheral blood was sampled from mice throughout *H. polygyrus* infection to assess circulatory monocyte counts by flow cytometry (CD45$^+$, Lin$^-$, CD11b$^+$, Ly6G$^-$, CD115$^+$, Fig. 2A). Elevated total monocyte numbers were observed from seven to ten days post infection (Fig. 2B) and their numbers returned to baseline by 14 days post infection. Circulatory monocytes in the mouse can be distinguished into three phenotypic subtypes; classical, intermediate and non-classical monocytes[25,26]. Using the markers Ly6C and Treml4 to separate these three populations (Fig. 2A), the *H. polygyrus* induced expansion of monocytes was found to be predominantly in Ly6C$^+$Treml4$^-$ classical monocytes (Fig. 2C).

H. polygyrus infection induces bone marrow monopoiesis.

Under normal physiological conditions, murine classical monocytes have a half-life of just over one day in the circulation, with constant replenishment from the bone marrow[27,28]. To understand if the monocytosis in blood during *H. polygyrus* infection reflected changes at the level of bone marrow haematopoiesis, we used colony forming assays to assess the progenitor lineage potential during*H. polygyrus* infection. Four days post infection there was an increase in the number of monocyte-committed progenitors (Colony Forming Unit – Monocytic; CFU-M) compared to uninfected controls (Fig. 3A). Although this elevation was short lived and lost by 10 dpi (Fig. 3B), enumeration of classical monocytes (Lin$^-$, CD16/CD32$^+$, CD117$^-$, CD115$^+$, Ly6C$^+$, Fig. 3C) in the bone marrow confirmed that their numbers increase in the context of *H. polygyrus* infection (Fig. 3D).

H. polygyrus infection induced increase in blood monocytes and lung mononuclear phagocytes is IFN-I signalling dependent.

IFN-I signalling through IFNAR is essential to the *H. polygyrus*induced anti-viral effect[6]. To test if the expansion in mononuclear phagocytes was dependent on this signalling axis, cell counts were assessed 10 dpi with H. polygyrus in*Ifnar1*$^{-/-}$ mice, which are maintained on a C57BL/6 background. Importantly, the *H. polygyrus* induced expansion of lung mononuclear phagocytes (Fig. 4A) and of circulatory monocytes (Fig. 4B) were evident in control C57BL/6 mice but lost in the absence of IFN-I signalling. In contrast, IFNAR-deficient mice still had increases in committed monocyte progenitors in the bone marrow after*H. polygyrus* , albeit to a lower level than in wild type controls. Ly6C$^+$ monocyte numbers in the bone marrow also seemed to increase after *H. polygyrus* , but without reaching statistical significance (Fig. 4C,D).

H. polygyrus monocytosis results in higher numbers of lung mononuclear phagocytes early after RSV infection.

RSV induced monocyte influx and subsequent accumulation of lung mononuclear phagocytes is crucial for the production of cytokines associated with the antiviral response[13]. To ascertain if this early influx was altered following *H. polygyrus*infection, we used flow cytometry to assess the monocyte-macrophage compartment eight hours post RSV infection. RSV infection alone increased the numbers of mononuclear phagocytes in the lung (Fig. 5A), as others have observed, but after prior infection with *H. polygyrus* their counts were significantly higher than after RSV infection alone (Fig. 5B). This expansion was seen in both Ly6C$^+$ and CD11c$^+$ macrophages (Fig. 5C,D). Four days after RSV infection, numbers of Ly6C$^+$macrophages remained higher in mice with prior *H. polygyrus*infection, while the increase in numbers of CD11c$^+$macrophages did

not persist (Fig. 5E). Alveolar macrophage numbers were unaffected by prior *H. polygyrus* infection at both 8 and 96 hours post RSV infection (Fig. S1A,B). These findings demonstrate that *H. polygyrus* infection leads to numbers of lung mononuclear phagocytes that exceed those found early after RSV infection alone, raising the possibility that high numbers of these cells confers an early protective effect against RSV infection.

Expanded circulatory monocytes are necessary and sufficient for enhanced immunity against RSV infection.

To assess if the *H. polygyrus*- induced increase in lung mononuclear phagocytes contributes to the previously reported *H. polygyrus* induced antiviral effect against RSV, monocytes were depleted through administration of anti-CCR2 (MC-21) antibodies seven and nine days after *H. polygyrus* infection. Flow cytometry analysis of tail vein blood 10 dpi confirmed that the antibody treatment reversed the expansion of circulatory monocytes, returning their numbers to steady state levels (Fig. 6A). Anti-CCR2 treatment also prevented the increases in mononuclear phagocytes (Fig. 6B), Ly6C$^+$macrophages (Fig. 6C) and CD11c$^+$ macrophages (Fig. 6D) in the lung. Alveolar macrophage numbers appeared to be unaffected by anti-CCR2 treatment, as expected for this tissue resident population without overt inflammatory stimuli (Fig. S1C). Mice were then intranasally infected with 10^5 pfu RSV and their lungs were assessed for viral load by immunoplaque assay four days post RSV infection (14 days after *H. polygyrus* infection). The RSV load was significantly reduced following *H. polygyrus* infection, as expected. However, anti-CCR2 treatment prevented this decrease in RSV load (Fig. 6E). This demonstrates that increases in circulatory monocytes and lung mononuclear phagocytes are required for the *H. polygyrus* induced protective effect against RSV infection.

Finally, to complement these depletion experiments we used adoptive monocyte transfer to test if elevated numbers of blood monocytes are sufficient to replicate the *H. polygyrus* effect and limit RSV infection. Female BALB/c mice were infected with *H. polygyrus* and ten days later bone marrow was isolated and enriched for monocytes to 94% using negative lineage selection beads to minimise monocyte activation. Two million monocytes from *H. polygyrus* infected or control mice were intravenously transferred to naïve mice to raise their number in the circulation immediately prior to RSV infection. Analysis of the peak viral load four days after RSV infection showed significant decreases in RSV titres after adoptive monocyte transfer from both control and *H. polygyrus* infected animals. Taken together, these data demonstrate that increasing the numbers of circulatory monocytes is sufficient to increase anti-RSV immunity irrespective of the infection state of the donors (Fig. 6F).

Discussion

H. polygyrus infection reduces RSV infection peak viral load, secondary immuno-pathology, and associated lung function impairment[6]. We now describe how this helminth infection induces enhanced monopoiesis in the bone marrow, elevated circulatory monocytes and increased recruitment of monocyte derived mononuclear phagocytes to the lung. Using monocyte ablation and transfer we show the functional importance of circulatory monocyte derived cells in the *H. polygyrus* -induced anti-viral effect against RSV. Elevated numbers of circulatory leukocytes over the first two weeks of *H. polygyrus* infection, including lymphocytes, neutrophils and monocytes have previously been described but only in C57BL/6 mice[29,30]. The correlative observations of bone marrow myelopoiesis to drive this expansion in circulatory monocytes, and the subsequent elevation of lung mononuclear phagocytes are novel to our study. We expect that the mononuclear phagocyte population in the lung is directly derived from circulatory monocytes. This is supported by the circulatory increase being observed from 7 dpi, whereas lung mononuclear phagocytes remain unchanged until 10 dpi. The absence of the increase in lung mononuclear phagocytes when circulatory monocytes are ablated supports this interpretation. However, due to the potential for persistence of CCR2 on tissue mononuclear phagocytes[31] we cannot discount the possibility that we directly ablated cells in the lung as well.

A growing body of work has assessed the interplay between parasitic and viral infections[32]. *H. polygyrus* infection has been previously described to suppress influenza A (IAV) infections although the mechanism was undetermined[33]. *Trichinella spiralis* infection improves disease outcome to IAV in a gut damage dependent mechanism, but this was through suppression of secondary inflammation, rather than reduction in viral titres and no alteration in the mononuclear phagocyte compartment was observed[34]. *Schistosoma mansoni*

(*S. mansoni*) infection is protective against secondary infection with IAV and in pneumonia virus of mice (PVM) infection it gave a small reduction in peak PVM load[35]. *S. mansoni* larvae pass through the lung in mice so their effect on respiratory viral infection is likely due to local inflammatory responses rather than to the systemic response observed with the strictly enteric *H. polygyrus* . A mononuclear phagocyte response was not reported but others have described *S. mansoni* to drive recruitment of alternatively activated macrophages[36]. Their local immunosuppressive effect is often detrimental to viral infection control, with both*H. polygyrus* and *S. mansoni* infection reactivating latent murine γ-herpesvirus infections by suppressing the antiviral IFN response[37].

The promotion of alternative activated macrophages in helminth infection has also been described in tissues peripheral to the gut. *H. polygyrus* induces heart macrophages with a strong type 2 polarisation which appear at 28 dpi[38]. The absence of elevated blood monocytes at this late time point, and the very small increase in the number of monocytes and mononuclear phagocytes expressing the M2 marker CD301 (predominantly regulatory macrophages, data not shown) at 10 dpi in our study, further indicate that different mechanisms are responsible for the early induction of lung mononuclear phagocytes after*H. polygyrus* infection and a later type-2 immunity driven expansion of alternatively activated macrophages.

An active factor driving the early *H. polygyrus* effects observed in our study has not yet been identified but the fact that both the antiviral effect and the expansion of both blood monocytes and lung mononuclear phagocytes depend on IFNAR signalling likely implies a role for IFN-Is either as direct effectors or stimuli for a secondary signal. The monocytic response to IFN-I signalling is key to myeloid responses in many other infections. IFNAR-deficient mice have been used widely in SARS-CoV-2 models where this disruption impairs recruitment of Ly6C$^+$ monocytes to the lung[39,40]. In other inflammatory conditions this may be due to decreased turnover to Ly6C$^-$ monocytes, but the overall increase in total monocyte and mononuclear phagocyte numbers in *H. polygyrus*infection suggests other additional effects[14]. IFNAR signalling has also been linked to mononuclear phagocyte function in IAV infection[41,42] and to inflammatory monocyte accumulation in mucosal herpes simplex virus infection[43]. IFN-I signalling is also key to the accumulation of inflammatory Ly6C$^+$ mononuclear phagocytes in the lung associated with older age, with a phenotype similar to that seen in viral infections such as IAV[44]. In PVM infection IFNAR signalling has no effect on monocytic cells but is required for the induction of inflammatory conventional dendritic cells, indicating a likely infection specificity of myeloid IFN-I signalling requirements[45]. However, dendritic cells express CD11c and may contribute to the CD11c$^+$ macrophages we have found to expand after*H. polygyrus* infection. Indeed the ongoing difficulty in characterising the mononuclear phagocyte sub-compartments in murine pulmonary inflammation (recently reviewed[46,47]) due to shared expression of the key markers used for steady state characterisation is also a limitation in this study. It is important to note that similar to the work in our study the use of global IFNAR knockouts in the studies above means that despite the usually high expression of IFNAR on monocytes, their response may be dependent on secondary cells.

Effects of IFN-Is on blood monocytes are less well studied including in*Ifnar1* deficiency. The historical characterisations of IFNAR-deficient mice showed elevated circulatory monocytes, counter to our model, but the increased risk of infection in IFNAR-deficient mice, at a time before modern infection control measures were available, may have contributed to this effect[20]. In human peripheral blood mononuclear cells (PBMCs) classical monocytes are more responsive to IFN-Is than non-classical monocytes due to differential abundance of IFNAR[48] and culture of PBMCs with IFN-Is will alter their phenotype[49-51]. An expansion of circulatory monocytes and lung CD64$^+$ cells, similar to our findings, was observed in idiopathic pulmonary fibrosis patients and associated with increased circulatory IFN-Is[52]. Exogenous treatment with IFNα for two to four weeks in asthma patients also increased the numbers of circulating monocytes and increased their antigen presenting phenotype[53].

Clearly, from the array of responses described above the context of IFN-I signalling is crucial. The outcome of IFN-I stimulation is modulated by concomitant signalling/environmental factors that certainly also play a role in *H. polygyrus* responses[54]. One such environmental factor is the microbiome and it's metabolic products, the presence of which is essential for the *H. polygyrus*antiviral effect[6]. While we were unable

to test the impact of the microbiome in the present study, interactions between IFN-I production and microbiome components have been well described[55,56] and the microbiome is known to be modulated in helminth infections including *H. polygyrus*infection[57,58].

The apparent lack of dependency on IFNAR signalling for bone marrow monopoiesis in this model suggests alternative signalling requirements. Interferon treatments have been described to affect lymphopoiesis[59], IFN-I suppresses neutrophil differentiation[60,61], and IFNγ promotes myelopoiesis[62,63]. Parasitic modulation of the bone marrow has also been described, with *Trichuris muris* and*Trichuris gondii* infections modulating haematopoiesis in an IFNγ dependent manner[64,65]. There is also substantial evidence that interferon regulatory factor 5 (IRF5) is a key regulator of hematopoietic development, particularly in myeloid lineages[66,67]. *H. polygyrus* has been recently described to induce IFN-γ (IFN-II) early in infection[68] which may be responsible for the initial induction of monopoiesis. The deeply interlinked feedback loops between IFN-I and IFN-II signalling may explain why we see a reduced effect on monocytosis in the bone marrow[69].

The mechanism of the anti-viral effect of *H. polygyrus* -induced mononuclear phagocytes is as yet unclear. In RSV infection mononuclear phagocytes are known to produce TNFα which is important for control of viral expansion, providing a possible mechanism[13] but their direct effects on viral load were not assessed. Our findings directly demonstrate, for the first time, that elevating mononuclear phagocyte numbers in the lung prior to RSV infection can reduce viral load. Monocytes/macrophages are also known to produce IFNβ, viperin and OAS in response to viral exposure, thus the expansion of mononuclear phagocytes in the lung may explain the previously observed increase in these antiviral factors in whole lung samples during *H. polygyrus*infection[19,70-73].

In conclusion, we show that intestinal helminth infection can induce transient systemic monocytosis and increased numbers of mononuclear phagocytes within the lung that are essential to reducing the burden of viral respiratory infection. Due to the IFNAR dependency of this expansion in the blood and lung we hypothesise that helminth induced IFN-Is or secondary signalling products play a key role in these effects. Future work will be required to identify the specific factors that act upon monocytes to drives these effects and to further characterise the specific anti-viral mechanisms of these cells in RSV infection.

References:

1. Estimates of the global, regional, and national morbidity, mortality, and aetiologies of lower respiratory infections in 195 countries, 1990-2016: a systematic analysis for the Global Burden of Disease Study 2016. *Lancet Infect Dis.*2018;18(11):1191-1210.

2. Falsey AR, Hennessey PA, Formica MA, Cox C, Walsh EE. Respiratory syncytial virus infection in elderly and high-risk adults. *N Engl J Med.* 2005;352(17):1749-1759.

3. Nguyen-Van-Tam JS, O'Leary M, Martin ET, et al. Burden of respiratory syncytial virus infection in older and high-risk adults: a systematic review and meta-analysis of the evidence from developed countries. *Eur Respir Rev.* 2022;31(166).

4. Binns E, Tuckerman J, Licciardi PV, Wurzel D. Respiratory syncytial virus, recurrent wheeze and asthma: A narrative review of pathophysiology, prevention and future directions.*J Paediatr Child Health.* 2022;58(10):1741-1746.

5. Soto JA, Stephens LM, Waldstein KA, Canedo-Marroquin G, Varga SM, Kalergis AM. Current Insights in the Development of Efficacious Vaccines Against RSV. *Front Immunol.*2020;11:1507.

6. McFarlane AJ, McSorley HJ, Davidson DJ, et al. Enteric helminth-induced type I interferon signaling protects against pulmonary virus infection through interaction with the microbiota. *J Allergy Clin Immunol.* 2017(140):1068-1078.

7. Maizels RM. Regulation of immunity and allergy by helminth parasites. *Allergy.* 2020;75(3):524-534.

8. Schoggins JW, Wilson SJ, Panis M, et al. A diverse range of gene products are effectors of the type I interferon antiviral response. *Nature.* 2011;472(7344):481-485.

9. Schoggins JW. Interferon-Stimulated Genes: What Do They All Do? *Annu Rev Virol.* 2019;6(1):567-584.

10. Sposito B, Broggi A, Pandolfi L, et al. The interferon landscape along the respiratory tract impacts the severity of COVID-19. *Cell.* 2021;184(19):4953-4968 e4916.

11. McNab F, Mayer-Barber K, Sher A, Wack A, O'Garra A. Type I interferons in infectious disease. *Nat Rev Immunol.* 2015;15(2):87-103.

12. Khaitov MR, Laza-Stanca V, Edwards MR, et al. Respiratory virus induction of alpha-, beta- and lambda-interferons in bronchial epithelial cells and peripheral blood mononuclear cells. *Allergy.* 2009;64(3):375-386.

13. Goritzka M, Makris S, Kausar F, et al. Alveolar macrophage-derived type I interferons orchestrate innate immunity to RSV through recruitment of antiviral monocytes. *J Exp Med.* 2015;212(5):699-714.

14. Lee PY, Li Y, Kumagai Y, et al. Type I interferon modulates monocyte recruitment and maturation in chronic inflammation. *Am J Pathol.* 2009;175(5):2023-2033.

15. Krausgruber T, Blazek K, Smallie T, et al. IRF5 promotes inflammatory macrophage polarization and TH1-TH17 responses. *Nat Immunol.* 2011;12(3):231-238.

16. Askenasy N. Interferon and tumor necrosis factor as humoral mechanisms coupling hematopoietic activity to inflammation and injury. *Blood Rev.* 2015;29(1):11-15.

17. Essers MA, Offner S, Blanco-Bose WE, et al. IFNalpha activates dormant haematopoietic stem cells in vivo.*Nature.* 2009;458(7240):904-908.

18. Dalmas E, Toubal A, Alzaid F, et al. Irf5 deficiency in macrophages promotes beneficial adipose tissue expansion and insulin sensitivity during obesity. *Nat Med.*2015;21(6):610-618.

19. Kim TH, Kim CW, Oh DS, Jung HE, Lee HK. Monocytes Contribute to IFN-beta Production via the MyD88-Dependent Pathway and Cytotoxic T-Cell Responses against Mucosal Respiratory Syncytial Virus Infection. *Immune Netw.*2021;21(4):e27.

20. Muller U, Steinhoff U, Reis LF, et al. Functional role of type I and type II interferons in antiviral defense. *Science.* 1994;264(5167):1918-1921.

21. Johnston CJ, Robertson E, Harcus Y, et al. Cultivation of Heligmosomoides polygyrus: an immunomodulatory nematode parasite and its secreted products. *J Vis Exp.*2015(98):e52412.

22. Currie SM, Findlay EG, McHugh BJ, et al. The human cathelicidin LL-37 has antiviral activity against respiratory syncytial virus. *PLoS One.* 2013;8(8):e73659.

23. Plantinga M, Guilliams M, Vanheerswynghels M, et al. Conventional and monocyte-derived CD11b(+) dendritic cells initiate and maintain T helper 2 cell-mediated immunity to house dust mite allergen. *Immunity.* 2013;38(2):322-335.

24. Hawley CA, Rojo R, Raper A, et al. Csf1r-mApple Transgene Expression and Ligand Binding In Vivo Reveal Dynamics of CSF1R Expression within the Mononuclear Phagocyte System.*J Immunol.* 2018;200(6):2209-2223.

25. Tacke F, Randolph GJ. Migratory fate and differentiation of blood monocyte subsets.*Immunobiology.* 2006;211(6-8):609-618.

26. Ingersoll MA, Spanbroek R, Lottaz C, et al. Comparison of gene expression profiles between human and mouse monocyte subsets. *Blood.* 2010;115(3):e10-19.

27. Yona S, Kim KW, Wolf Y, et al. Fate mapping reveals origins and dynamics of monocytes and tissue macrophages under homeostasis. *Immunity.* 2013;38(1):79-91.

28. Hettinger J, Richards DM, Hansson J, et al. Origin of monocytes and macrophages in a committed progenitor.*Nat Immunol.* 2013;14(8):821-830.

29. Ali NM, Behnke JM, Manger BR. The pattern of peripheral blood leucocyte changes in mice infected with Nematospiroides dubius. *J Helminthol.* 1985;59(1):83-93.

30. Baker NF. The nature and etiology of the leukocytic response of Webster mice infected with Nematospiroides dubius. *J Parasitol.* 1962;48:438-441.

31. Dick SA, Wong A, Hamidzada H, et al. Three tissue resident macrophage subsets coexist across organs with conserved origins and life cycles. *Sci Immunol.*2022;7(67):eabf7777.

32. Desai P, Diamond MS, Thackray LB. Helminth-virus interactions: determinants of coinfection outcomes.*Gut Microbes.* 2021;13(1):1961202.

33. Chowaniec W, Wescott RB, Congdon LL. Interaction of Nematospiroides dubius and influenza virus in mice.*Exp Parasitol.* 1972;32(1):33-44.

34. Furze RC, Hussell T, Selkirk ME. Amelioration of influenza-induced pathology in mice by coinfection with Trichinella spiralis. *Infect Immun.* 2006;74(3):1924-1932.

35. Scheer S, Krempl C, Kallfass C, et al. S. mansoni bolsters anti-viral immunity in the murine respiratory tract. *PLoS One.* 2014;9(11):e112469.

36. Santos MP, Goncalves-Santos E, Goncalves RV, et al. Doxycycline aggravates granulomatous inflammation and lung microstructural remodeling induced by Schistosoma mansoni infection. *Int Immunopharmacol.* 2021;94:107462.

37. Reese TA, Wakeman BS, Choi HS, et al. Helminth infection reactivates latent gamma-herpesvirus via cytokine competition at a viral promoter. *Science.* 2014;345(6196):573-577.

38. Mylonas KJ, Jenkins SJ, Castellan RF, et al. The adult murine heart has a sparse, phagocytically active macrophage population that expands through monocyte recruitment and adopts an 'M2' phenotype in response to Th2 immunologic challenge.*Immunobiology.* 2015;220(7):924-933.

39. Ogger PP, Garcia Martin M, Michalaki C, et al. Type I interferon receptor signalling deficiency results in dysregulated innate immune responses to SARS-CoV-2 in mice.*Eur J Immunol.* 2022;52(11):1768-1775.

40. Channappanavar R, Fehr AR, Vijay R, et al. Dysregulated Type I Interferon and Inflammatory Monocyte-Macrophage Responses Cause Lethal Pneumonia in SARS-CoV-Infected Mice. *Cell Host Microbe.* 2016;19(2):181-193.

41. Garcia-Sastre A, Durbin RK, Zheng H, et al. The role of interferon in influenza virus tissue tropism.*J Virol.* 1998;72(11):8550-8558.

42. Price GE, Gaszewska-Mastarlarz A, Moskophidis D. The role of alpha/beta and gamma interferons in development of immunity to influenza A virus in mice. *J Virol.*2000;74(9):3996-4003.

43. Lee AJ, Chen B, Chew MV, et al. Inflammatory monocytes require type I interferon receptor signaling to activate NK cells via IL-18 during a mucosal viral infection. *J Exp Med.* 2017;214(4):1153-1167.

44. D'Souza SS, Zhang Y, Bailey JT, et al. Type I Interferon signaling controls the accumulation and transcriptomes of monocytes in the aged lung. *Aging Cell.*2021;20(10):e13470.

45. Bosteels C, Neyt K, Vanheerswynghels M, et al. Inflammatory Type 2 cDCs Acquire Features of cDC1s and Macrophages to Orchestrate Immunity to Respiratory Virus Infection. *Immunity.* 2020;52(6):1039-1056 e1039.

46. Aegerter H, Lambrecht BN, Jakubzick CV. Biology of lung macrophages in health and disease. *Immunity.* 2022;55(9):1564-1580.

47. T'Jonck W, Bain CC. The role of monocyte-derived macrophages in the lung: It's all about context. *Int J Biochem Cell Biol.* 2023;159:106421.

48. Han S, Zhuang H, Lee PY, et al. Differential Responsiveness of Monocyte and Macrophage Subsets to Interferon. *Arthritis Rheumatol.* 2020;72(1):100-113.

49. Pogue SL, Preston BT, Stalder J, Bebbington CR, Cardarelli PM. The receptor for type I IFNs is highly expressed on peripheral blood B cells and monocytes and mediates a distinct profile of differentiation and activation of these cells. *J Interferon Cytokine Res.* 2004;24(2):131-139.

50. Dickensheets HL, Donnelly RP. Inhibition of IL-4-inducible gene expression in human monocytes by type I and type II interferons. *J Leukoc Biol.* 1999;65(3):307-312.

51. Tong Y, Zhou L, Yang L, et al. Concomitant type I IFN and M-CSF signaling reprograms monocyte differentiation and drives pro-tumoral arginase production. *EBioMedicine.* 2019;39:132-144.

52. Fraser E, Denney L, Antanaviciute A, et al. Multi-Modal Characterization of Monocytes in Idiopathic Pulmonary Fibrosis Reveals a Primed Type I Interferon Immune Phenotype. *Front Immunol.* 2021;12:623430.

53. Simon HU, Seelbach H, Ehmann R, Schmitz M. Clinical and immunological effects of low-dose IFN-alpha treatment in patients with corticosteroid-resistant asthma. *Allergy.* 2003;58(12):1250-1255.

54. van Boxel-Dezaire AH, Rani MR, Stark GR. Complex modulation of cell type-specific signaling in response to type I interferons. *Immunity.* 2006;25(3):361-372.

55. Winkler ES, Shrihari S, Hykes BL, Jr., et al. The Intestinal Microbiome Restricts Alphavirus Infection and Dissemination through a Bile Acid-Type I IFN Signaling Axis. *Cell.* 2020;182(4):901-918 e918.

56. Erttmann SF, Swacha P, Aung KM, et al. The gut microbiota prime systemic antiviral immunity via the cGAS-STING-IFN-I axis. *Immunity.* 2022;55(5):847-861 e810.

57. Kennedy MHE, Brosschot TP, Lawrence KM, et al. Small Intestinal Levels of the Branched Short-Chain Fatty Acid Isovalerate Are Elevated during Infection with Heligmosomoides polygyrus and Can Promote Helminth Fecundity. *Infect Immun.* 2021;89(12):e0022521.

58. Reynolds LA, Smith KA, Filbey KJ, et al. Commensal-pathogen interactions in the intestinal tract: lactobacilli promote infection with, and are promoted by, helminth parasites. *Gut Microbes.* 2014;5(4):522-532.

59. Di Scala M, Gil-Farina I, Vanrell L, et al. Chronic exposure to IFNalpha drives medullar lymphopoiesis towards T-cell differentiation in mice. *Haematologica.*2015;100(8):1014-1022.

60. Siakaeva E, Pylaeva E, Spyra I, et al. Neutrophil Maturation and Survival Is Controlled by IFN-Dependent Regulation of NAMPT Signaling. *Int J Mol Sci.* 2019;20(22).

61. Nguyen-Jackson H, Panopoulos AD, Zhang H, Li HS, Watowich SS. STAT3 controls the neutrophil migratory response to CXCR2 ligands by direct activation of G-CSF-induced CXCR2 expression and via modulation of CXCR2 signal transduction. *Blood.* 2010;115(16):3354-3363.

62. Grainger JR, Wohlfert EA, Fuss IJ, et al. Inflammatory monocytes regulate pathologic responses to commensals during acute gastrointestinal infection. *Nat Med.*2013;19(6):713-721.

63. Buechler MB, Akilesh HM, Hamerman JA. Cutting Edge: Direct Sensing of TLR7 Ligands and Type I IFN by the Common Myeloid Progenitor Promotes mTOR/PI3K-Dependent Emergency Myelopoiesis. *J Immunol.* 2016;197(7):2577-2582.

64. Chenery AL, Antignano F, Hughes MR, Burrows K, McNagny KM, Zaph C. Chronic Trichuris muris infection alters hematopoiesis and causes IFN-gamma-expressing T-cell accumulation in the mouse bone marrow. *Eur J Immunol.* 2016;46(11):2587-2596.

65. Askenase MH, Han SJ, Byrd AL, et al. Bone-Marrow-Resident NK Cells Prime Monocytes for Regulatory Function during Infection. *Immunity.* 2015;42(6):1130-1142.

66. Schoenemeyer A, Barnes BJ, Mancl ME, et al. The interferon regulatory factor, IRF5, is a central mediator of toll-like receptor 7 signaling. *J Biol Chem.*2005;280(17):17005-17012.

67. Corbin AL, Gomez-Vazquez M, Berthold DL, et al. IRF5 guides monocytes toward an inflammatory CD11c(+) macrophage phenotype and promotes intestinal inflammation.*Sci Immunol.* 2020;5(47).

68. Progatzky F, Shapiro M, Chng SH, et al. Regulation of intestinal immunity and tissue repair by enteric glia. *Nature.* 2021;599(7883):125-130.

69. Michalska A, Blaszczyk K, Wesoly J, Bluyssen HAR. A Positive Feedback Amplifier Circuit That Regulates Interferon (IFN)-Stimulated Gene Expression and Controls Type I and Type II IFN Responses. *Front Immunol.* 2018;9:1135.

70. Nasr N, Maddocks S, Turville SG, et al. HIV-1 infection of human macrophages directly induces viperin which inhibits viral production. *Blood.* 2012;120(4):778-788.

71. Lee D, Le Pen J, Yatim A, et al. Inborn errors of OAS-RNase L in SARS-CoV-2-related multisystem inflammatory syndrome in children. *Science.*2023;379(6632):eabo3627.

72. Fagone P, Nunnari G, Lazzara F, et al. Induction of OAS gene family in HIV monocyte infected patients with high and low viral load. *Antiviral Res.* 2016;131:66-73.

73. Teng TS, Foo SS, Simamarta D, et al. Viperin restricts chikungunya virus replication and pathology.*J Clin Invest.* 2012;122(12):4447-4460.

Figure Legends:

Fig 1. *H. polygyrus*infection induces an expansion of lung mononuclear phagocytes. Female BALB/c mice were administered an equal volume of either sterile dH_2O as infection control (i) or 200 *H. polygyrus*(H. poly) L3 larvae (ii) by oral gavage. Seven, 10, and 14 days post infection (dpi) lungs were harvested for flow cytometry analysis. (A) Representative gating strategy for the identification of alveolar macrophages ($CD45^+$, $Ly6G^-$, $SigF^+$, $CD64^+$) and mononuclear phagocytes ($CD45^+$, $Ly6G^-$, $SigF^-$, $CD11b^+$, $CD64^+$). (B-C) Absolute numbers of (B) mononuclear phagocytes and (C) alveolar macrophages at the indicated time points post *H. polygyrus* infection. (D) Representative expression of Ly6C and CD11c by lung $SigF^-$, $CD11b^+$, $CD64^+$ cells obtained from *H. polygyrus* infected mice at 10 dpi. (E-F) Absolute numbers of (E) $Ly6C^+CD11c^-$ and (F) $Ly6C^-CD11c^+$ mononuclear phagocytes at the indicated time points post H. polygyrus infection. Symbols represent individual mice with n=6 per group pooled from two independent experiments. Statistical significance of difference determined with unpaired two-tailed t-test. $^*P < 0.05$, $^{***}P < 0.001$.

Fig 2. *H. polygyrus* infection induces circulatory monocytosis. Female BALB/c mice were administered an equal volume of either sterile dH_2O as infection control (i) or 200 *H. polygyrus*(H. poly) L3 larvae (ii) by oral gavage. (A) Flow cytometry to identify monocytes ($CD45^+$, $Lineage^-$, $CD11b^+$, $Ly6G^-$, $CD115^+$), and the monocytic subsets – classical ($Ly6C^+$, $Treml4^-$) intermediate ($Ly6C^+$, $Treml4^+$), and non-classical ($Ly6C^-$, $Treml4^+$) (B) Monocyte numbers per mL blood at indicated time points post *H. polygyrus*infection. (C) Numbers of blood monocyte subtypes 10 dpi with *H. polygyrus* . Symbols represent individual mice with n=6 per group pooled from two independent experiments. Statistical significance of difference determined with unpaired two-tailed t-test. $^{**}P < 0.01$, $^{***}P < 0.001$.

Fig 3. *H. polygyrus* infection induces bone marrow monopoiesis. Female BALB/c mice were administered an equal volume of either sterile dH_2O as infection control (i) or 200 *H. polygyrus*(H. poly) L3 larvae (ii) by oral

gavage. (A) Bone marrow colony forming assays (CFAs) were performed on hind limb bone marrow 4 dpi, assessing monocytic colony forming units (CFU-M) blast forming unit – erythroid (BFU-E), colony forming unit granulocytic (CFU-G), granulocytic/monocytic (CFU-GM), granulocytic/erythroid/monocytic mixed (GEMM). (B) The increase in CFU-M subsides by 10 dpi. (C) Flow cytometry analysis of bone marrow characterised bone marrow monocytes (lineage$^-$, CD16/CD32$^+$, CD117$^-$, CD115$^+$, Ly6C$^+$). (D) Numbers of bone marrow monocytes were assessed throughout *H. polygyrus* infection. Symbols represent individual mice n=4 for control and n=6 for *H. polygyrus* groups pooled from two independent CFU experiments. Flow cytometry experiments day 4 and 7 n=6 per group, day 10 n = 9 per group. Statistical significance of difference determined with unpaired two-tailed t-test. $*P$ <0.05, $**P$ <0.01.

Fig 4. IFNAR signalling is essential *for H. polygyrus*induced blood monocyte and lung mononuclear phagocyte expansion but not bone marrow monopoiesis. Female C57BL/6 or *Ifnar1-/-* mice were administered 200 *H. polygyrus* L3 larvae by oral gavage or an equal volume of sterile dH_2O as infection control. 10 dpi lungs were harvested for flow cytometry analysis. Across C56BL/6 and Ifnar1-/- mice numbers of (A) lung mononuclear phagocytes (B) blood monocytes and (C) bone marrow Lyc6$^+$ monocytes were assessed. (D) Bone marrow colony forming assays (CFAs) were assessed from hind limb bone marrow 10 dpi (other CFA outputs non-significant). Symbols represent individual mice with n=6 per group pooled from two independent experiments for lung. One experiment of n=4 per group for blood and bone marrow. Statistical significance of difference determined with one way ANOVA $*P$ <0.05, ** P <0.01, $***P$ <0.001, $****P$ <0.0001.

Fig 5. *H. polygyrus* infection accelerates accumulation of mononuclear phagocytes in early RSV infection. (A) Female BALB/c mice were ntranasally administered 10^5 pfu RSV then culled 8 hours later and numbers of lung mononuclear phagocytes were assessed by flow cytometry. (B-E) Female BALB/c mice were administered *H. polygyrus* (H. poly) or dH_2O infection control by oral gavage and ten days later infected intranasally with 10^5 pfu RSV. Eight hours after RSV infection lungs were analysed by flow cytometry to assess numbers of (B) lung mononuclear phagocytes, (C) Ly6C$^+$ macrophages and (D) CD11c$^+$ macrophages. (E) Macrophage subsets were also assessed 96 hours post RSV administration with and without prior*H. polygyrus* infection. Symbols represent individual mice with n=6 per group pooled from two independent experiments. Statistical significance of difference determined with unpaired two-tailed t-test. $*P$ <0.05, $*P$ <0.0001.

Fig 6. Circulatory monocytes are necessary and sufficient for the anti-RSV effects of *H. polygyrus* infection. Female BALB/c mice were administered *H. polygyrus* (H. poly) or dH_2O as a control by oral gavage. At 7 and 9 dpi the*H. polygyrus* infected animals were administered MC-21 anti-CCR2 antibody via IP injection. (A) Blood monocyte counts at 10 dpi. A subset of mice were culled at 10 dpi to assess numbers of (B) mononuclear phagocytes, (C) Ly6C$^+$ macrophages and (D) CD11C$^+$ macrophages in the lung. All remaining mice were infected intranasally with 10^5 pfu RSV. (E) Four days post RSV infection viral load was assessed by immunoplaque assays. (F) Bone marrow was collected from female BALB/c mice 10 dpi with*H. polygyrus* or dH_2O as a control. Samples were enriched for bone marrow monocytes using magnetic bead negative lineage selection and 2 million monocytes administered intravenously via the tail vein 30 minutes prior to RSV inoculation. PBS was used as a control for monocyte administration. Viral load at 4 dpi RSV was assessed by immunoplaque assay. Symbols represent individual mice with n=6 per group pooled from two independent experiments for RSV infection. For dual infection n=11 across two independent experiments with four samples taken for lung flow cytometry analysis and remainders for viral load assessment. Eight mice across two experiments for monocyte transfer experiment. Statistical significance of difference determined by one-way ANOVA with multiple comparisons. $*P$ <0.05, ** P <0.01, $****P$ <0.0001. Counts in (B-D) log transformed prior to statistical analysis.

Fig S1. Alveolar macrophages in *H. polygyrus* and respiratory syncytial virus infections. Female BALB/c mice were administered *H. polygyrus* (H. poly) or dH_2O infection control by oral gavage and ten days later infected intranasally with 10^5 pfu RSV. Alveolar macrophage numbers assessed at (A) 8 hours and (B) 96 hours post RSV infection. Female BALB/c mice were administered *H. polygyrus* (H. poly) or

dH_2O as a control by oral gavage. At 7 and 9 dpi the *H. polygyrus* infected animals were administered MC-21 anti-CCR2 antibody via IP injection. (C) Alveolar macrophage numbers assessed 10 dpi. Symbols represent individual mice with n=6 per group pooled from two independent experiments for H. polygyrus RSV coinfections. For MC21 treatment n=4 per group pooled from two independent experiments. All groups no significant differences.

End:

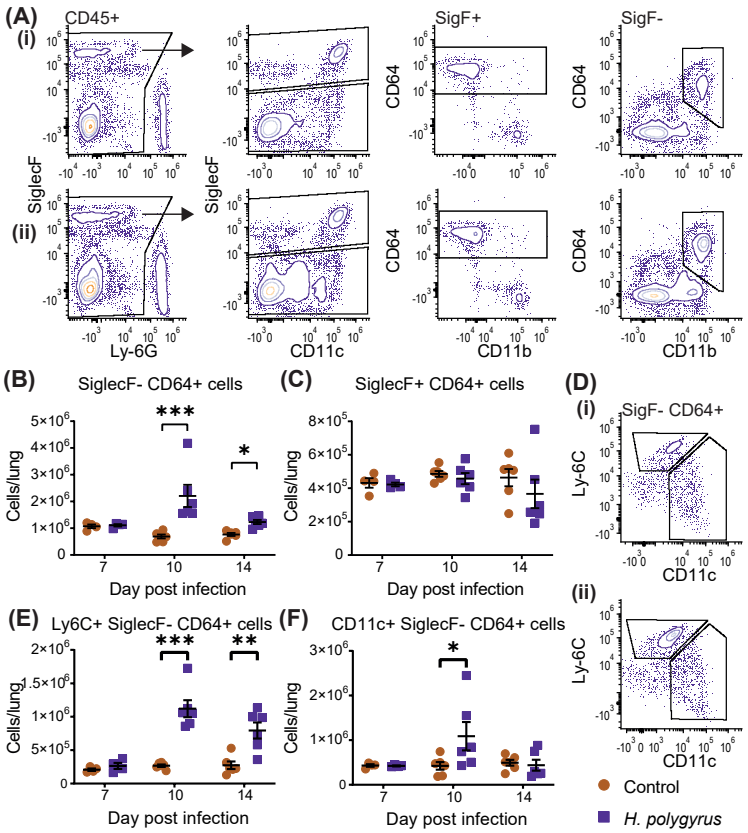

Figure 1_Burgess et al.

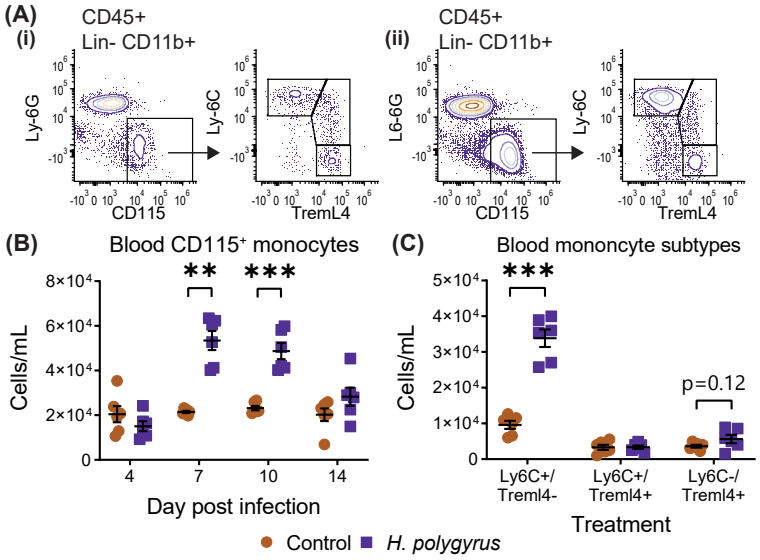

Figure 2_Burgess et al.

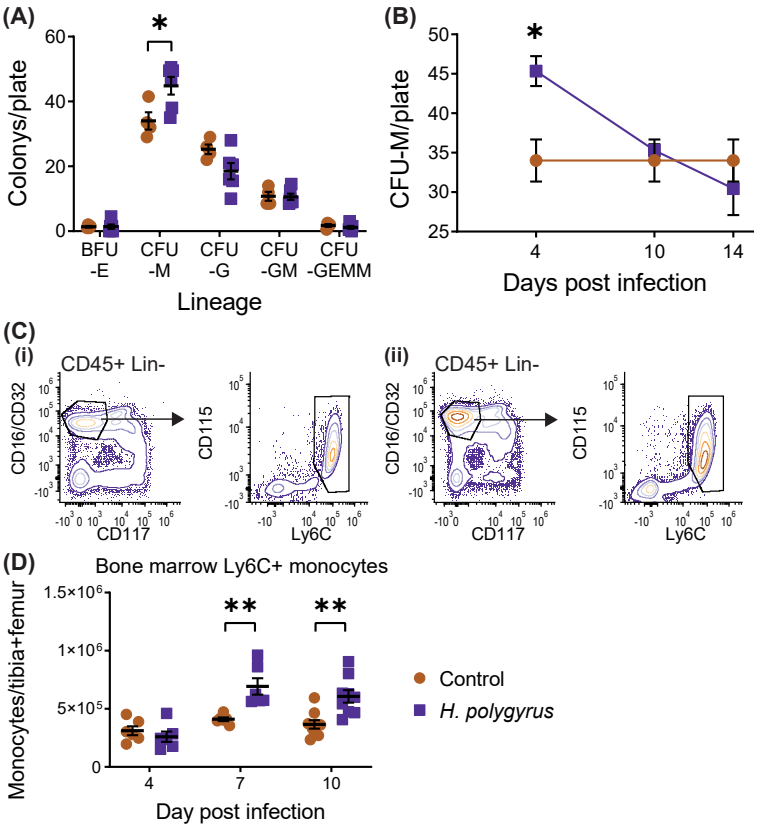

Figure 3_Burgess et al.

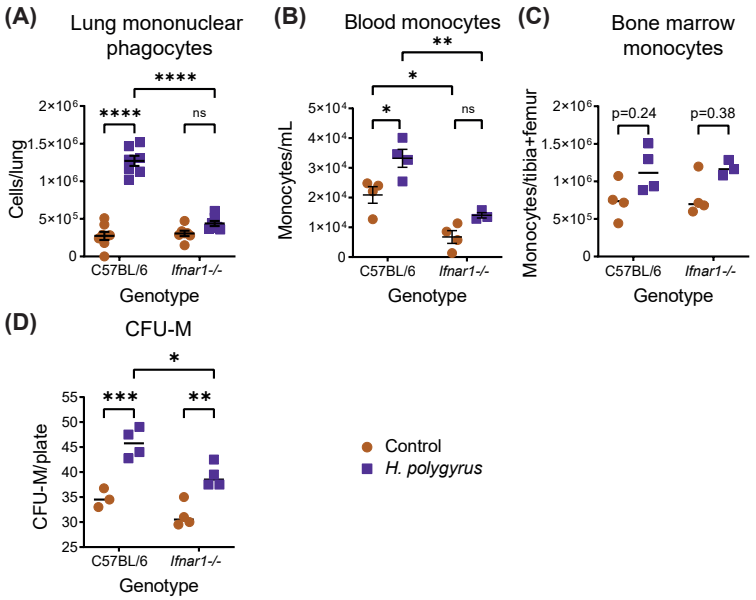

Figure 4_Burgess et al.

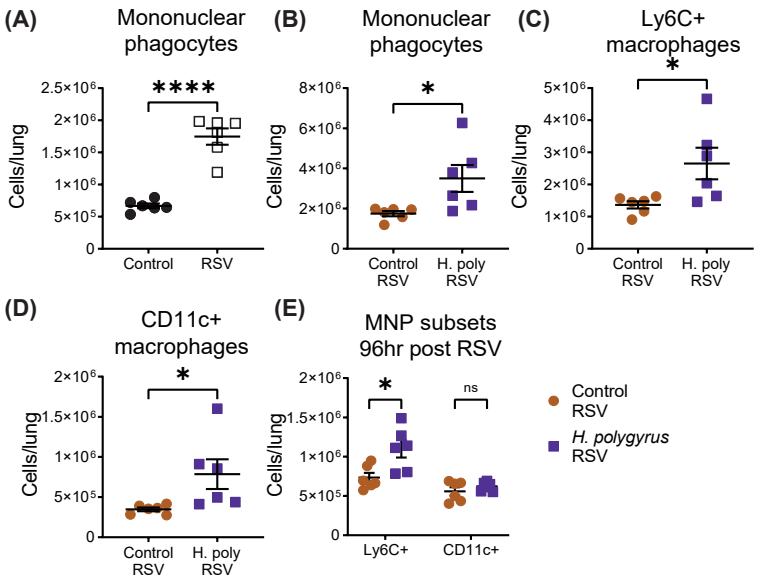

Figure 5_Burgess et al.

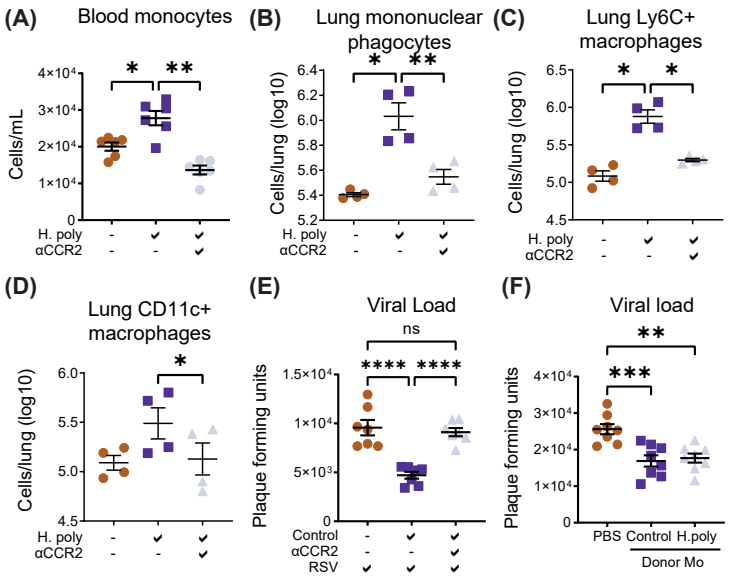

Figure 6_Burgess et al.